Journal of Molecular Spectroscopy 257 (2009) 20–23

Contents lists available at ScienceDirect

Journal of Molecular Spectroscopy

journal homepage: www.elsevier.com/locate/jms

Revised molecular constants and term values for the $X^2\Pi$ and $B^2\Sigma^+$ states of OH

Peter F. Bernath [a,*], Reginald Colin [b]

[a] Department of Chemistry, University of York, Heslington, York YO10 5DD, UK
[b] Service de Chimie Quantique et Photophysique, Université Libre de Bruxelles (ULB), 50, av. F.D. Roosevelt, 1050 Brussels, Belgium

ARTICLE INFO

Article history:
Received 19 May 2009
Available online 13 June 2009

Keywords:
Spectroscopy
Radicals
Solar spectra
Nightglow

ABSTRACT

An improved set of molecular constants and term values are given for the $X^2\Pi$ ($v = 0$–13) and $B^2\Sigma^+$ ($v = 0$ and 1) states of the OH radical. They are derived from a fit of previously published laboratory data and additional lines taken from infrared solar spectra recorded on orbit.

1. Introduction

OH is the most important free radical in the Earth's atmosphere because it cleans the troposphere of accumulated organic molecules that would otherwise rapidly accumulate and poison us [1]. It is also found in energetic environments such as flames [2] and in a wide variety of astronomical sources such as comets [3], stellar atmospheres [4] including the Sun [5], interstellar clouds [6] and planetary atmospheres [7] via microwave (Λ-doubling), pure rotational, vibration–rotation and electronic transitions. Our primary focus in this paper is on the vibration–rotation bands often called the Meinel system (or Meinel bands) from their observation in the night sky by Meinel [8].

The Meinel system is a prominent feature in the nighttime airglow of the Earth's atmosphere [8,9]. This nightglow originates in the upper mesosphere near 87 km from the reaction of hydrogen atoms with ozone, which populates high vibrational levels (up to $v = 9$) of the ground $X^2\Pi$ state [9]. The Meinel system is useful in atmospheric science because the bands show evidence of gravity wave structure seen, for example, in all sky airglow images [10]. These airglow emissions are also used to derive rotational temperatures by taking appropriate ratios of line intensities and provide valuable information about the mesosphere [11]. The Meinel system can also be studied from orbit and the SABER emission radiometer instrument on the TIMED satellite is currently monitoring the OH airglow through two near infrared filters at 1.6 and 2 μm [12].

In astronomy, the Meinel bands are generally a nuisance because they interfere with faint astronomical observations in the visible and near infrared regions, although they are occasionally used for wavelength calibration. Recently Cosby et al. [13] have prepared a very useful high resolution atlas of the nightglow emissions.

The best available set of molecular constants and term values for the ground $X^2\Pi$ state of the OH molecule is essentially based on two papers. The first is that of Mélen et al. [14] who, in 1995, gathered all the spectroscopic data available at that time from laboratory and satellite [15] (ATMOS 1985) measurements involving the $v = 0$–3 vibrational levels of this important radical and fitted them to a standard $^2\Pi$ Hamiltonian. A set of term values were thus generated which allowed the calculation of the line positions for any infrared band involving these vibrational levels. These lines were often used later for calibration of other IR spectra. The second paper is that of Colin et al. [16], in which the measurements obtained by Abrams et al. [17] of 17 IR bands involving $v = 4$–10 were refitted to generate molecular constants and term values for these higher vibrational levels. In that fit, the molecular constants for the levels $v = 0$–3 given by Mélen et al. [14] were kept constant.

In the course of a detailed examination of the IR and far IR bands of OH present in older (ATMOS 1985 [15], ATMOS 1994 [18]) and more recent (ACE [19]) satellite solar absorption spectra, it was found that there existed a discrepancy between the observed line positions and those calculated with the above mentioned constants. For the pure rotational $v = 0$ band the discrepancy, less than 0.001 cm^{-1} for lines with $J < 24.5$, reached 0.14 cm^{-1} for lines with $J = 49.5$. The discrepancy is most likely due to a faulty Λ-doubling matrix element in the $^2\Pi$ Hamiltonian used by Mélen et al. [14]. A refitting of all available spectroscopic data appeared necessary on account of the importance of this radical in many fields of molecular science. In addition, in the course of our inspection of the various satellite solar spectra, 29 previously missing lines and several

* Corresponding author. Fax: +44 (0) 1904 432516.
E-mail address: pfb500@york.ac.uk (P.F. Bernath).

0022-2852/$ - see front matter © 2009 Elsevier Inc. All rights reserved.
doi:10.1016/j.jms.2009.06.003

high J lines of the so far unobserved $v = 4$ pure rotational band were found. In addition, data from the literature was used to extend our work to $v = 13$ of the $X^2\Pi$ state.

2. Data and analysis

The $^2\Pi$ Hamiltonian used in this work is that of Brown et al. [20] along with a partial list of matrix elements provided by Amiot et al. [21]. The necessary additional higher order matrix elements were generated by algebraic multiplication using the Maple program. The fitting program used was limited to a maximum of 90 fitted molecular constants. Therefore the fitting procedure was done in four steps.

In fit A, all the measurements available in the literature concerning exclusively the $v = 0$, 1, 2 and 3 levels of the $X^2\Pi$ state were treated. The data used in this fit are given in Table 1 with their references. In addition to the pure rotation bands 0–0, 1–1, 2–2 and 3–3 taken from Mélen et al. [14], eleven infrared bands measured by Mélen et al. [14], Abrams et al. [17] or Maillard et al. [22] were used. Our fitting program cannot accommodate hyperfine structure resolved data such as those given by Mélen et al. [14] in their Table IB1 and IB2. These very precise data for low J values of $v = 0$, 1, 2 and 3 were nevertheless taken into account by introducing into the fit the Λ-doubling separations of the corresponding J values taken from the calculated term value table of Mélen et al. [14] (Table V). The weights given to the latter data were ten times greater than the pure rotation data which in turn were weighted ten times more than infrared measurements.

Fit B concerns the $v = 4$ level and includes all data involving $v = 4$ and lower vibrational levels (see Table 1). In this fit, all the constants relative to $v = 1$, 2 and 3 were fixed to their value obtained in fit A. Pure rotational lines for $v = 4$ with high J values, identified here for the first time in the ATMOS 1994 [18] spectrum, were used and are given in Table 2. The portion of the spectrum concerned was recalibrated using Mélen et al.'s [14] pure rotational bands as standards. Four of these very weak lines are shown in Fig. 1.

Fit C is a refit of all the infrared bands measured by Abrams et al. [17] and the 5–2 band measured by Maillard et al. [22]. When a choice was possible, the measurements of Abrams et al. were preferred to those of Maillard et al. because, in spite of the fact that the former end at lower J values than the latter, they are more precise. In this fit the constants for $v = 2$, 3 and 4 were fixed to the values obtained in fits A and B.

Table 1
Overview of the OH $X^2\Pi$ spectroscopic data used in the present analysis.

Fit A	Vibration-rotation	1–0, 2–1, 3–2	[14]
		1–0, 2–0, 2–1	[17]
		3–1, 3–2	[17]
		2–0, 3–0, 3–1	[22]
	Pure rotation	$v = 0$, 1, 2, 3	[14]
	Λ-doubling	$v = 0$, 1, 2, 3	See text
Fit B	Vibration-rotation	4–1	[22]
		4–2, 4–3	[17]
	Pure rotation	$v = 4$	This work
Fit C	Vibration-rotation	5–2	[22]
		5–3, 5–4, 6–4,	[17]
		6–5, 7–4, 7–5,	[17]
		7–6, 8–5, 8–6,	[17]
		8–7, 9–6, 9–7,	[17]
		9–8, 10–8, 10–9	[17]
Fit D	Vibration-rotation	11–9	[24]
		12–8	[25]
	Electronic $B^2\Sigma^+$–$X^2\Pi$	0–7, 0–8, 0–9,	[23]
		0–11, 0–12,	[23]
		0–13, 1–9	[23]

Table 2
Pure rotational lines of the $v = 4$ level of OH $X^2\Pi$ (cm^{-1}).

J	R_{2f}	R_{2e}	R_{1f}	R_{1e}
21.5	–	641.136	–	–
22.5	–	661.705	641.859	640.945
23.5	680.601	681.386	662.362	661.472
24.5	699.370	700.134	–	681.099
25.5	717.196	717.945	700.680	699.823
26.5	734.049	734.758	718.439	717.610
27.5	749.882	750.577	735.208	734.428
28.5	–	–	750.981	750.239
29.5	778.449	779.051	–	–
30.5	791.089	791.641	779.379	–
31.5	–	–	791.937	–

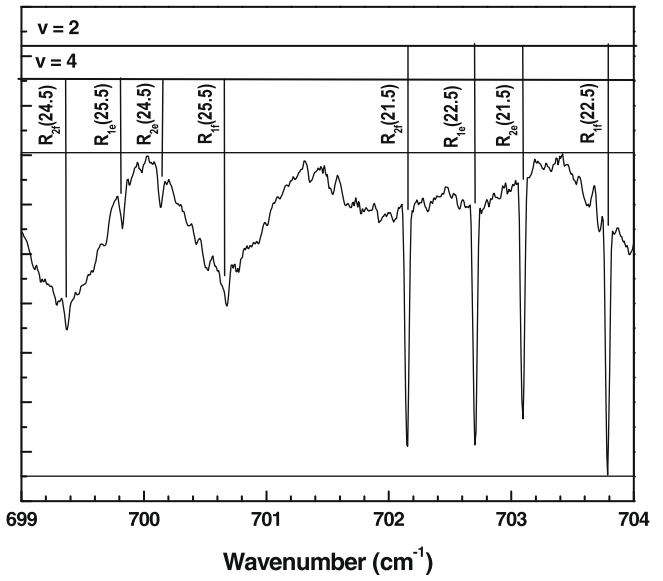

Fig. 1. A portion of the OH pure rotation spectrum for $v = 2$ and 4 seen in the solar infrared spectrum recorded by ATMOS [18].

Fit D concerns the $v = 11$, 12 and 13 levels of the $X^2\Pi$ state. It contains the $B^2\Sigma^+$–$X^2\Pi$ electronic bands with $v' = 0$ and 1 available in the literature [23] and the infrared $X^2\Pi$ (11–9) [24] and (12–8) [25] bands.

3. Results and discussion

In all, 3679 lines were fitted yielding 189 constants for 14 vibrational levels of the $X^2\Pi$ state (Table 3) and 12 constants for the first two levels of the $B^2\Sigma^+$ state (Table 4).

Term values for the $v = 0$–13 levels of the $X^2\Pi$ state and of the $v = 0$ and 1 levels of the $B^2\Sigma^+$ state of OH are available on ScienceDirect (www.sciencedirect.com) and as part of the Ohio State University Molecular Spectroscopy Archives (http://msa.lib.ohio-state.edu/jmsa_hp.htm). These term values are extrapolated to five J values above the last observed rotational level. For the $v = 0$ level for which the highest J value is 49.5, no extrapolated values are given. A list giving all the spectroscopic measurements used in this work along with the observed–calculated values obtained is also available on this site.

An atlas of terrestrial nightglow emission lines from spectra of the night sky obtained from the Ultraviolet and Visual Echelle Spectrograph (UVES) on the Very Large Telescope (VLT) facility in Chile has been published [13]. It contains 1254 lines that have been

Table 3
Molecular constants for the $X^2\Pi$ state of OH (cm^{-1}).

v	0	1	2	3	4	5	6
T	0	3570.35227(13)	6975.09355(12)	10216.14778(16)	13294.61451(17)	16210.59982(17)	18962.99243(19)
A	−139.050901)	−139.32036(13)	−139.586866(89)	−139.843998(99)	−140.08244(45)	−140.28876(42)	−140.43893(46)
B	18.5348674(37)	17.8239239(35)	17.1224747(37)	16.4279052(44)	15.7370129(47)	15.0456206(86)	14.348658(11)
$D \times 10^3$	1.908916(27)	1.870458(27)	1.835804(31)	1.805942(41)	1.782650(29)	1.76638(12)	1.76163(17)
$H \times 10^7$	1.42643(68)	1.37750(68)	1.31836(86)	1.2441(13)	1.16286(50)	0.9961(55)	0.8452(92)
$L \times 10^{11}$	−1.4690(79)	−1.5690(75)	−1.692(10)	−1.822(17)	−2.1241(27)	−1.416(82)	−1.75(15)
$M \times 10^{15}$	0.879(47)	1.250(38)	1.693(56)	2.01(10)	[2.5]	[2.8]	[3.1]
$N \times 10^{20}$	6.2(14)	−8.80(71)	−32.6(11)	−66.0(23)	[−100]	[−100]	[−100]
$O \times 10^{23}$	−3.96(16)	[−4.0]	[−4.0]	[−4.0]	[−4.0]	–	–
$\gamma \times 10$	−1.19171(42)	−1.13736(40)	−1.08277(40)	−1.02636(47)	−0.96915(82)	−0.9048(11)	−0.8401(12)
$\gamma_D \times 10^5$	2.315(19)	2.294(15)	2.297(16)	2.334(23)	2.522(47)	2.55(12)	3.13(14)
$\gamma_H \times 10^9$	−2.81(17)	−2.472(74)	−2.070(84)	−1.83(15)	−3.48(40)	−6.4(36)	−17.1(40)
$\gamma_L \times 10^{13}$	3.51(43)	[3.5]	[3.5]	[3.5]	[3.5]	–	–
$q \times 10^2$	−3.86886(12)	−3.69375(17)	−3.51788(18)	−3.33886(25)	−3.15793(70)	−2.96972(42)	−2.77765(81)
$q_D \times 10^5$	1.4708(13)	1.4462(18)	1.4263(14)	1.4012(21)	1.3975(50)	1.3802(23)	1.404(10)
$q_H \times 10^9$	−2.635(19)	−2.606(35)	−2.601(16)	−2.485(30)	−2.473(91)	[−2.5]	−2.75(28)
$q_L \times 10^{13}$	3.757(99)	4.02(26)	4.438(54)	4.68(12)	4.79(50)	–	–
$q_M \times 10^{17}$	−2.02(17)	−2.08(61)	[−2.0]	[−2.0]	[−2.0]	–	–
$p \times 10$	2.35285(15)	2.24713(23)	2.13949(30)	2.02910(44)	1.91485(87)	1.79496(57)	1.66572(62)
$p_D \times 10^5$	−5.261(25)	−5.217(34)	−5.203(36)	−5.235(37)	−5.339(64)	−5.681(42)	−5.973(50)
$p_H \times 10^9$	7.71(37)	7.20(62)	6.45(61)	5.15(26)	3.80(65)	[3.5]	[2.8]
$p_L \times 10^{12}$	−2.80(19)	−2.88(45)	−3.20(24)	[−3.0]	[−3.0]	–	–
v	7	8	9	10	11	12	13
T	21549.17731(21)	23964.63990(24)	26202.44582(25)	28252.53784(47)	30100.8113(39)	31728.2549(48)	33109.6609(39)
A	−140.50361(51)	−140.42967(47)	−140.14026(52)	−139.50575(75)	−138.3257(84)	−136.3610(96)	−133.0318(66)
B	13.639333(11)	12.908879(21)	12.145344(20)	11.332573(42)	10.45015(41)	9.45851(52)	8.32781(31)
$D \times 10^3$	1.77067(17)	1.80050(55)	1.85785(49)	1.95724(99)	2.1368(60)	2.346(12)	2.7908(51)
$H \times 10^7$	0.6010(91)	0.337(53)	−0.111(41)	−0.717(64)	[−1.5]	[−2.5]	[−4.0]
$L \times 10^{11}$	−1.74(15)	−3.4(17)	−5.8(11)	[−12.5]	–	–	–
$M \times 10^{15}$	[3.4]	[3.7]	[4.0]	[4.3]	–	–	–
$N \times 10^{20}$	[−100]	[−100]	[−100]	[−100]	–	–	–
$O \times 10^{23}$	–	–	–	–	–	–	–
$\gamma \times 10$	−0.7614(14)	−0.6718(12)	−0.5559(13)	−0.4015(15)	−0.291(36)	0.433(35)	0.868(20)
$\gamma_D \times 10^5$	3.22(17)	4.022(90)	5.17(10)	[6.0]	[7.0]	[8.5]	[10.0]
$\gamma_H \times 10^9$	−17.7(52)	[−30.0]	[−60]	[−100]	–	–	–
$\gamma_L \times 10^{13}$	–	–	–	–	–	–	–
$q \times 10^2$	−2.57291(89)	−2.35662(86)	−2.1187(11)	−1.8586(10)	−1.570(43)	−1.285(31)	−0.723(19)
$q_D \times 10^5$	1.406(12)	1.4547(76)	1.489(10)	[1.59]	[1.7]	[1.8]	[1.9]
$q_H \times 10^9$	−2.69(34)	[−3.0]	[−3.3]	[−3.6]	–	–	–
$q_L \times 10^{13}$	–	–	–	–	–	–	–
$q_M \times 10^{17}$	–	–	–	–	–	–	–
$p \times 10$	1.52229(70)	1.36198(90)	1.1689(10)	0.9354(23)	0.503(32)	0.303(20)	−0.57(13)
$p_D \times 10^5$	−6.443(64)	−7.41(10)	−8.20(12)	−9.32(49)	[−12.0]	[−18.0]	[−27.0]
$p_H \times 10^9$	[1.8]	[1.0]	–	–	–	–	–
$p_L \times 10^{12}$	–	–	–	–	–	–	–

Values in brackets were kept fixed in the fit.

Table 4
Molecular constants for the $B^2\Sigma^+$ state of OH (cm^{-1}).

v	T	B	$D \times 10^3$	$H \times 10^6$	$\gamma \times 10^2$	$\gamma_D \times 10^4$
0	68386.6375(19)	5.08776(48)	0.929(43)	−0.380(28)	2.637(53)	−0.393(92)
1	69046.4688(44)	4.10190(54)	2.082(19)	−9.79(18)	2.17(14)	−1.38(31)

identified as belonging to the Meinel OH bands. As none of these observed nightglow lines has $J'' > 24.5$, the former identifications, based on the older term values [14,16], remain unchanged. Nevertheless, all of the identifications were checked with the present new term values and found to be satisfactory, although the nightglow line positions derived from our new spectroscopic constants and term values are more accurate.

A convenient source of Meinel band line positions and intensities has been the HITRAN 2004 [26] database, which is based primarily on the calculations of Goldman et al. [27]. Unfortunately the spectroscopic constants used to generate the line positions for higher J values do not reproduce the observations [17]. This has been rectified by Goldman for the latest 2008 edition of HITRAN [28] using a preliminary version of the term values presented in this paper.

Acknowledgments

The research in Belgium was funded by the FRS-FNRS, the Belgian State Federal Office for Scientific, Technical and Cultural Affairs and the European Space Agency (ESA-Prodex arrangements C90-327). Financial support by the Actions de Recherche Concertées (Communauté Française de Belgique) is also acknowledged. Some support was provided by the UK Engineering and Physical Sciences Research Council (EPSRC) and the NASA laboratory astrophysics program.

Appendix A. Supplementary data

Supplementary data for this article are available on ScienceDirect (www.sciencedirect.com) and as part of the Ohio State University Molecular Spectroscopy Archives (http://library.osu.edu/sites/msa/jmsa_hp.htm).

References

[1] J. Lelieveld, F.J. Dentener, W. Peters, M.C. Krol, Atmos. Chem. Phys. 4 (2004) 2337–2344.
[2] T.B. Settersten, R.L. Farrow, J.A. Gray, Chem. Phys. Lett. 369 (2003) 584–590.
[3] N. Dello Russo, M.J. Mumma, M.A. DiSanti, K. Magee-Sauer, E.L. Gibb, B.P. Bonev, I.S. McLean, L.-H. Xu, Icarus 184 (2006) 255–276.
[4] J. Meléndez, B. Barbuy, Astrophys. J. 575 (2002) 474–483.
[5] M. Asplund, N. Grevesse, A.J. Sauval, C. Allende Prieto, D. Kiselman, Astron. Astrophys. 417 (2004) 751–768.
[6] J.R. Goicoechea, J. Cernicharo, Astrophys. J. 576 (2002) L77–L81.
[7] G. Piccioni, P. Drossart, L. Zasova, A. Migliorini, J.-C. Gérard, F.P. Mills, A. Shakun, A. García Muñoz, N. Ignatiev, D. Grassi, V. Cottini, F.W. Taylor, S. Erard, Astron. Astrophys. 483 (2008) L29–L33.
[8] A.B. Meinel, Astrophys. J. 111 (1950) 555–564. 112 (1950) 120–130.
[9] P.C. Cosby, T.G. Slanger, Can. J. Phys. 85 (2007) 77–99.
[10] H.U. Frey, S.B. Mende, J.F. Arens, P.R. McCullough, G.R. Swenson, Geophys. Res. Lett. 27 (2000) 41–44.
[11] F.J. Mulligan, R.P. Lowe, Ann. Geophys. 26 (2008) 1–17.
[12] M. López-Puertas, M. García-Comas, B. Funke, R.H. Picard, J.R. Winick, P.P. Wintersteiner, M.G. Mlynczak, C.J. Mertens, J.M. Russell III, L.L. Gordley, J. Geophys. Res. 109 (2004) D09307, doi:10.1029/2003JD004383.
[13] P.C. Cosby, B.D. Sharpee, T.G. Slanger, D.L. Huestis, R.W. Hanuschik, J. Geophys. Res. 111 (2006) A12307, doi:10.1029/2006JA012023.
[14] F. Mélen, A.J. Sauval, N. Grevesse, C.B. Farmer, Ch. Servais, L. Delbouille, G. Roland, J. Mol. Spectrosc. 174 (1995) 490–509.
[15] C. B. Farmer, R.H. Norton, Atlas of the Infrared Spectrum of the Sun and the Earth Atmosphere from Space, vol. I: The Sun, NASA Ref. Pub. 1224, NASA, Washington, DC, 1989; M. Geller, Atlas of the Infrared Spectrum of the Sun and the Earth Atmosphere from Space, vol. III: Key to Identification of Solar Features, NASA Ref. Pub. 1224, NASA, Washington, DC, 1992.
[16] R. Colin, P.-F. Coheur, M. Kiseleva, A.C. Vandaele, P.F. Bernath, J. Mol. Spectrosc. 214 (2002) 225–226.
[17] M.C. Abrams, S.P. Davis, M.L.P. Rao, R. Engleman, J.W. Brault, Astrophys. J. Suppl. Ser. 93 (1994) 351–395.
[18] M.C. Abrams, A. Goldman, M.R. Gunson, C.P. Rinsland, R. Zander, Appl. Opt. 35 (1996) 2747–2751.
[19] P.F. Bernath, C.T. McElroy, M.C. Abrams, C.D. Boone, M. Butler, C. Camy-Peyret, M. Carleer, C. Clerbaux, P.-F. Coheur, R. Colin, P. DeCola, M. De Mazière, J.R. Drummond, D. Dufour, W.F.J. Evans, H. Fast, D. Fussen, K. Gilbert, D.E. Jennings, E.J. Llewellyn, R.P. Lowe, E. Mahieu, J.C. McConnell, M. McHugh, S.D. McLeod, R. Michaud, C. Midwinter, R. Nassar, F. Nichitiu, C. Nowlan, C.P. Rinsland, Y.J. Rochon, N. Rowlands, K. Semeniuk, P. Simon, R. Skelton, J.J. Sloan, M.-A. Soucy, K. Strong, P. Tremblay, D. Turnbull, K.A. Walker, I. Walkty, D.A. Wardle, V. Wehrle, R. Zander, J. Zou, Geophys. Res. Lett. 32 (2005) L15S01, doi:10.1029/2005GL022386.
[20] J.M. Brown, E.A. Colbourne, J.K.G. Watson, F.D. Wayne, J. Mol. Spectrosc. 74 (1979) 294–318.
[21] C. Amiot, J.-P. Maillard, J. Chauville, J. Mol. Spectrosc. 87 (1981) 196–218.
[22] J.P. Maillard, J. Chauville, A.W. Mantz, J. Mol. Spectrosc. 63 (1976) 120–141.
[23] R.A. Copeland, B.R. Chalamala, J.A. Coxon, J. Mol. Spectrosc. 161 (1993) 243–252.
[24] S.A. Nizkorodov, W.W. Harper, D.J. Nesbitt, Chem. Phys. Lett. 341 (2001) 107–114.
[25] A.D. Sappey, R.A. Copeland, J. Mol. Spectrosc. 143 (1990) 160–168.
[26] L.S. Rothman, D. Jacquemart, A. Barbe, D.C. Benner, M. Birk, L.R. Brown, M.R. Carleer, C. Chackerian Jr., K. Chance, L.H. Coudert, V. Dana, V.M. Devi, J.-M. Flaud, R.R. Gamache, A. Goldman, J.-M. Hartmann, K.W. Jucks, A.G. Maki, J.-Y. Mandin, S.T. Massie, J. Orphal, A. Perrin, C.P. Rinsland, M.A.H. Smith, J. Tennyson, R.N. Tolchenov, R.A. Toth, J. Vander Auwera, P. Varanasi, G. Wagner, J. Quant. Spectrosc. Rad. Transfer 96 (2005) 139–204.
[27] A. Goldman, W.G. Schoenfeld, D. Goorvitch, C. Chackerian Jr., H. Dothe, I.F. Melen, M.C. Abrams, J.E.A. Selby, J. Quant. Spectrosc. Rad. Transfer 59 (1998) 453–469.
[28] L.S. Rothman, I.E. Gordon, A. Barbe, D.C. Benner, P.F. Bernath, M. Birk, V. Boudon, L.R. Brown, A. Campargue, J.-P. Champion, K. Chance, L.H. Coudert, V. Dana, V.M. Devi, S. Fally, J.-M. Flaud, R.R. Gamache, A. Goldman, D. Jacquemart, I. Kleiner, N. Lacome, W.J. Lafferty, J.-Y. Mandin, S.T. Massie, S.N. Mikhailenko, C.E. Miller, N. Moazzen-Ahmadi, O.V. Naumenko, A.V. Nikitin, J. Orphal, V.I. Perevalov, A. Perrin, A. Predoi-Cross, C.P. Rinsland, M. Rotger, M. Šimečková, M.A.H. Smith, K. Sung, S.A. Tashkun, J. Tennyson, R.A. Toth, A.C. Vandaele, J. Vander Auwera, J. Quant. Spectrosc. Rad. Transfer 110 (2009) 533–572.